

# Angular dependence of the order-disorder transition in proton irradiated single crystal MgB<sub>2</sub>

J. D. Moore,<sup>1</sup> G. K. Perkins,<sup>1</sup> A. D. Caplin,<sup>1</sup> J. Jun,<sup>2</sup> S. M. Kazakov,<sup>2</sup> J. Karpinski,<sup>2</sup> and L. F. Cohen<sup>1</sup>

<sup>1</sup>Blackett Laboratory, Imperial College, London SW7 2BZ, United Kingdom

<sup>2</sup>Solid State Physics Laboratory, ETH, CH-8093 Zürich, Switzerland

(Received 3 February 2005; published 21 June 2005)

We present magnetization results on a proton irradiated MgB<sub>2</sub> single crystal that displays a peak in magnetization for the field applied parallel to the *c* axis. Magnetic history effects are observed, which are ascribed to the occurrence of a disorder driven phase transition close to an inflection point in the magnetization-field curve. We demonstrate that the angular and temperature dependence of this feature is significantly different to that of the lower and upper critical fields.

DOI: 10.1103/PhysRevB.71.224509

PACS number(s): 74.70.Ad, 74.25.Op, 74.25.Qt, 74.62.Dh

## I. INTRODUCTION

The vortex state of type-II superconductors is bound by the lower and upper critical fields. Over recent years, vortex phenomenology has increased in complexity, particularly the recognition of other phase transitions in the field-temperature plane. For example, study of cuprate superconductors has shown there to be a melting transition from vortex solid to vortex liquid.<sup>1</sup>

Both low-temperature superconductors and the cuprates have an order-disorder transition from a Bragg glass to a highly disordered glassy phase.<sup>2-6</sup> This transition is accompanied by a peak in magnetization close to the upper critical field  $H_{c2}$ , known as the peak effect. One explanation of the peak effect is that the vortex lattice deforms plastically to occupy more pinning sites thus increasing the critical current density.<sup>7</sup> The transition also displays a metastable field region in magnetization loops that is dependent on the field and temperature history. The magnetic history effects are a distinctive signature of a disorder-driven first-order phase transition.<sup>4</sup>

The disorder induced peak effect has been observed in MgB<sub>2</sub> crystals<sup>8-10</sup> (which is an interesting material in its own right because of the two band nature of the superconductivity).<sup>11</sup> In a previous work,<sup>8</sup> crystals were studied that had naturally occurring disorder that was relatively weak. In these crystals a sharp peak effect was observed using torque magnetometry and it was found that the angular dependence of the onset to the peak and the maximum of the peak fields were similar to that of the upper critical field. The present work demonstrates that in a heavily disordered MgB<sub>2</sub> crystal, the temperature and angular dependence of the order-disorder phase transition are remarkably different to that of the upper and lower critical fields.

## II. EXPERIMENT

A MgB<sub>2</sub> virgin single crystal,<sup>12</sup> with approximate dimensions  $500\ \mu\text{m} \times 300\ \mu\text{m} \times 30\ \mu\text{m}$  and critical temperature  $T_c \approx 38\ \text{K}$ , was characterized by determining the lower critical field  $H_{c1}$  and the upper critical field  $H_{c2}$ . The crystal was subsequently proton irradiated with the aim of increasing the density of pinning centers and of enhancing  $H_{c2}$  and the criti-

cal current density. Fifteen consecutive implants were performed with beam energies varied between 400 keV and 2 MeV at a fluence of  $10^{16}\ \text{cm}^{-2}$ . Using a damage profile calculation originally created for a polycrystalline fragment, we can estimate that the proton irradiation induced pointlike disorder with a fairly uniform profile of approximately 1% dpa (displacements per atom) throughout the thickness of the crystal.<sup>13</sup>

A peak effect was observed in magnetization-field loops ( $M$ - $H$ ) near  $H_{c2}$ , but  $H_{c1}$  and  $H_{c2}$  remained unchanged. Characterization 3 months after irradiation showed that  $H_{c2}$  for the field parallel to the *c* axis ( $\mathbf{H} \parallel c$ ) had increased, and the peak effect was enhanced due to stronger pinning over a wide field range. These dramatic changes in the  $M$ - $H$  loop caused by postirradiation aging are described in detail elsewhere.<sup>14</sup> Here we report on magnetization measurements focusing on the peak effect transition with the applied magnetic field, taken during a 1 month period, 6 months after irradiation where no further change to the  $M$ - $H$  loop is observed when compared to the 3-month results.<sup>14</sup>

$M$ - $H$  loops were taken in an Oxford Instruments transverse vibrating sample magnetometer (TVSM) with a maximum magnetic field of 4 T. Data were measured at temperatures between 5 and 36 K as a function of the angle  $\theta$  between the *c* axis and the applied field  $H$ . The crystal *c* axis was aligned to within 1 deg of the field direction by detecting the reversal of magnetic moment orthogonal to the field direction.<sup>15</sup>

The lower critical field for  $\mathbf{H} \parallel c$  ( $H_{c1 \parallel c}$ ) was measured from the onset of remnant magnetization after successively higher swept field cycles. A full description of the method along with consideration of demagnetizing effects is described elsewhere.<sup>12</sup>

Magnetic history effects were explored by performing minor  $M$ - $H$  loops in the vicinity of the low-field side of the magnetic peak.<sup>4</sup> The field was increased from a negative starting value and then reversed at a point about the peak, thus forming a partial or *minor*  $M$ - $H$  loop. The opposite case, where the field is decreased from above  $H_{c2}$  and again reversed at the desired field, was also performed. A third case for investigating the metastable state was set out by first cooling in field from above  $T_c$  and then cycling the field up and down by 50 mT to produce several minor  $M$ - $H$  loops.

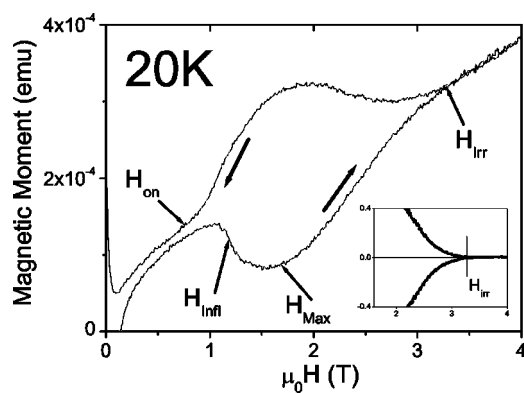


FIG. 1. A magnetization-field loop measured in a TVSM at 20 K and  $\mathbf{H}\parallel c$ . A broad peak in magnetization can be seen. The onset to the peak  $H_{on}$ , an inflection point of the peak  $H_{infl}$ , the maximum of the peak  $H_{max}$ , and the irreversibility field  $H_{irr}$  are labeled. Inset is a similar loop measured with a VHM. The TVSM signal includes a substantial, but reproducible, sloping instrumental background: the VHM signal is background free.

### III. RESULTS

First, we show the temperature and angular dependence of the lower critical field, the upper critical and characteristic fields associated with the peak effect. An investigation of the field-induced history effects around the peak in magnetization is then presented.

A representative  $M$ - $H$  loop is shown in Fig. 1 for  $\mathbf{H}\parallel c$  at 20 K. The peak effect is recognized as the enhanced magnetization hysteresis between 1 and 3.3 T. Various fields are labeled in Fig. 1, which are extracted from the magnetization hysteresis  $\Delta m$ . The onset field to the peak is labeled  $H_{on}$ ; the field where the maximum hysteresis in  $\Delta m$  occurs is labeled  $H_{max}$ ; an inflection in the slope where  $d(\Delta m)/dH$  is a maximum is labeled  $H_{infl}$ ; and the irreversibility field, defined to be where the hysteresis drops below the noise floor  $10^{-6}$  emu, is labelled  $H_{irr}$ .

In virgin crystals, a kink is apparent in the reversible magnetization as  $H_{c2}$  is approached. In this disordered crystal no kink can be seen at fields above  $H_{irr}$  (see Fig. 1). However, the large background signal at high fields in the TVSM can make this reversible feature hard to distinguish, so for these measurements  $H_{c2}$  was also extracted using a vibrating Hall micromagnetometer<sup>12</sup> (VHM) where the background signal is extremely low. The inset to Fig. 1 shows a magnified section of the main  $M$ - $H$  loop measured with the VHM at the same temperature and field alignment as the main figure. As can be seen  $\Delta m$  disappears at  $H_{irr}$  and there is no evidence of reversible magnetization above  $H_{irr}$ . This suggests the coincidence of  $H_{irr}$  and  $H_{c2}$  in the crystal.

The TVSM measures the global magnetic moment of the sample, whereas the VHM uses a  $20 \times 20 \mu\text{m}^2$  sized, InSb Hall sensor to measure the magnetic induction from an area less than 1% of the sample surface. Magnetization results performed using these two methods, and with the Hall sensor positioned at different points on the sample, showed  $M$ - $H$  loop shapes and  $H_{c2\parallel c}$  values that agree. This suggests the peak effect feature shown in Fig. 1 is representative of the

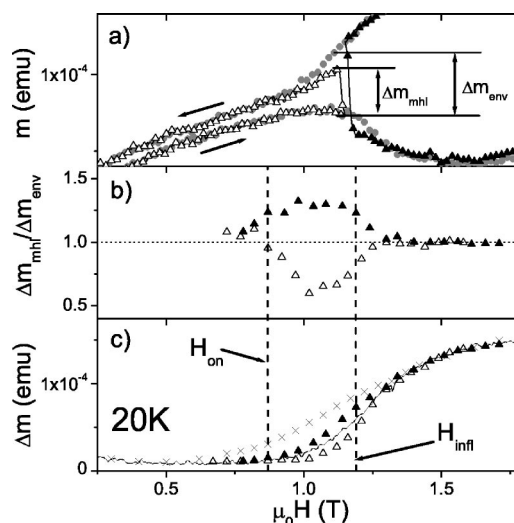


FIG. 2. (a) shows MHL for the field approaching from below  $MHL_{\uparrow}$  ( $\Delta$ ) and from above  $MHL_{\downarrow}$  ( $\blacktriangle$ ) along with the full envelope loop (gray circle) at 20 K and the field 20 deg to the  $c$  axis. Also shown are the extracted hysteresis widths  $\Delta m_{mhl}$  and  $\Delta m_{env}$  for the  $MHL_{\uparrow}$  and envelope loops, respectively. (b) shows the ratio  $\Delta m_{mhl}/\Delta m_{env}$  for the  $MHL_{\uparrow}$  and  $MHL_{\downarrow}$  data with the horizontal dotted line being the case of no magnetic history effects. (c) displays the magnetization hysteresis  $\Delta m$  for easy comparison of the  $MHL_{\uparrow}$  ( $\Delta$ ),  $MHL_{\downarrow}$  ( $\blacktriangle$ ), field cooled (FC) ( $\times$ ) and envelope loops (full line). The vertical dashed lines mark the onset to the peak  $H_{on}$  and the inflection point of the peak  $H_{infl}$ .

bulk sample and not due to any localized nature artifact introduced to the crystal during the irradiation and aging process.

The onset to the peak  $H_{on}$ , an inflection point of the peak  $H_{infl}$ , and the maximum of the peak  $H_{max}$ , have slightly different values on the increasing and decreasing field legs, and are also influenced by the background signal. For this reason the magnetization hysteresis was calculated, i.e., the reverse field leg minus the forward field leg and the characteristic fields of the peak are then extracted from this curve.

We determined the presence of magnetic history effects by taking minor hysteresis loops (MHL) in the vicinity of the magnetization peak. Figure 2(a) shows MHLs about  $H_{infl}$  at 20 K for the field 20 deg from the  $c$  axis. Magnetic history effects are observed as undershoot for the field increasing case  $MHL_{\uparrow}$ , and overshoot for the field decreasing case  $MHL_{\downarrow}$  when compared to the full magnetization or envelope loop. Figure 2(b) shows the ratio of the MHL and envelope loop hysteresis,  $\Delta m_{mhl}$  and  $\Delta m_{env}$ , respectively, as extracted in Fig. 2(a). A value other than unity indicates the presence of magnetic history effects. As can be seen in Fig. 2(b), the history effects extend to fields covering  $H_{on}$  and  $H_{infl}$ , but not at fields above  $H_{max}$ .

The field cooled MHLs consisted of several cycled loops of 50 mT excursions. The first loop cycle showed the greatest overshoot in the increasing and decreasing field legs with subsequent loops following the envelope curve. Figure 2(c) shows the magnetization hysteresis  $\Delta m$  for the field cooled loops,  $MHL_{\uparrow}$ ,  $MHL_{\downarrow}$  and the envelope curve along with  $H_{on}$  and  $H_{infl}$ . The field cooled magnetic history effects show a

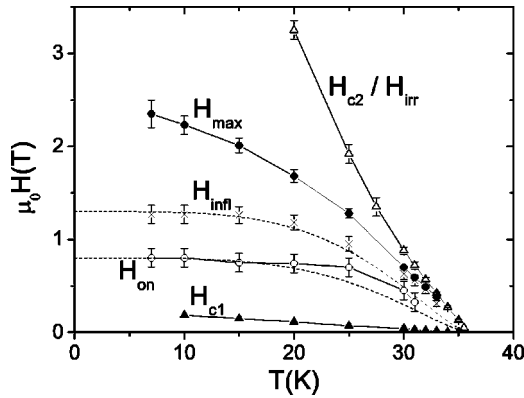


FIG. 3.  $H$ - $T$  phase diagram for  $\mathbf{H}\parallel c$ . The lower critical field  $H_{c1}$  ( $\blacktriangle$ ), the onset to the peak  $H_{on}$  ( $\circ$ ), an inflection point of the peak  $H_{infl}$  ( $\times$ ), the maximum of the peak  $H_{max}$  ( $\bullet$ ) and the upper critical field  $H_{c2}$  ( $\triangle$ ) are shown. Full lines are guides to the eye only. The dashed lines are data fits to Eq. (1) that is described in Sec. IV.

greater  $\Delta m$  that extends to lower fields than those for the  $MHL_{\uparrow}$  and  $MHL_{\downarrow}$  cases.

Figure 3 shows the  $H$ - $T$  phase diagram of  $H_{c1}$ ,  $H_{on}$ ,  $H_{infl}$ ,  $H_{max}$ , and  $H_{c2}$  for  $\mathbf{H}\parallel c$ .  $H_{c1}(T)$  has linear temperature dependence over the measured temperature range.  $H_{c2}(T)$  has a linear slope near  $T_c$  that becomes steeper between 20 and 30 K. Extrapolation of  $H_{c2}(T)$  gives the critical temperature  $T_c=36$  K.  $H_{on}$ ,  $H_{infl}$ , and  $H_{max}$  can be extracted up to temperatures  $\sim 33$  K, above which the peak effect has dropped below the noise level.  $H_{on}(T)$  and  $H_{infl}(T)$  have a negative curvature roughly above 20 K, but are temperature independent at lower temperatures.  $H_{max}(T)$  has a slight negative curvature throughout the temperature range. Note that  $H_{on}$  and  $H_{infl}$  show similar temperature dependence, which contrasts strongly with  $H_{c2}(T)$ . The dotted line is a fit of the  $H_{on}(T)$  and  $H_{infl}(T)$  curves to the order-disorder transition model by Giller *et al.*<sup>5</sup> Deviations from the predicted behavior occur at high temperature and may be a result of thermal effects which are intentionally neglected in the original Giller *et al.* model. The temperature dependence of the transition field is not dissimilar to that of the peak onset field in the highly anisotropic high temperature superconductor  $Ba_2Sr_2CaC_2O_6$  (BSCCO) system. In that system the onset of the peak has been interpreted in terms of a disorder induced transition from a relatively ordered vortex lattice to a highly disordered entangled vortex solid.<sup>16–18</sup> The temperature independent part of the onset field curve has been described as a two-dimensional (2D)-three-dimensional (3D) crossover in the vortex structure of BSCCO<sup>19</sup> or as a matching effect.<sup>20</sup> These latter descriptions are likely to be unique to BSCCO and other highly anisotropic superconductors.

Figure 4 shows  $H_{on}$ ,  $H_{infl}$ ,  $H_{max}$ , and  $H_{c2}$  as a function of field angle  $\theta$  from the  $c$  axis at 20 K. As  $\theta$  was tilted towards the  $ab$  plane, the peak simultaneously moved to higher field, broadened in field and the irreversible magnetization decreased. For the  $ab$ -plane field alignment, no peak was visible at any temperature and  $H_{on}$ ,  $H_{infl}$ , and  $H_{max}$  were not measurable. Likewise, measurement of the upper critical field in the  $ab$ -plane  $H_{c2\parallel ab}$  was not possible due to the signal's rapid diminution above the lower critical field. Figure 4

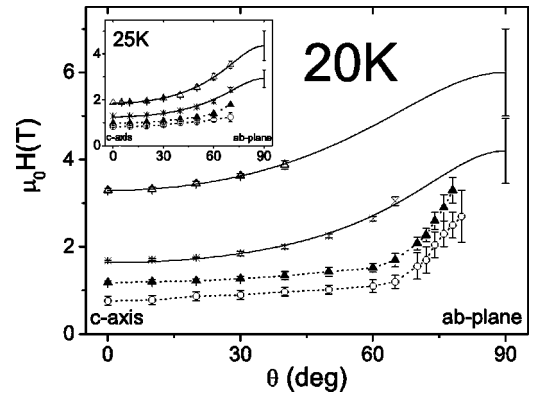


FIG. 4. The upper critical field  $H_{c2}$  ( $\triangle$ ), the maximum of the peak  $H_{max}$  ( $\times$ ), the peak inflection  $H_{infl}$  ( $\blacktriangle$ ) and the onset to the peak  $H_{on}$  ( $\circ$ ) as a function of the field angle  $\theta$  at 20 K. The full lines are data fits to the anisotropic Ginzburg-Landau theory and the dotted lines are guides to the eye. Inset is similar data taken at 25 K.

shows  $H_{max}$  and  $H_{c2}$  gradually increase over the measured angular range. In contrast,  $H_{on}$  and  $H_{infl}$  are nearly constant for  $\theta$  between 0 and 60 deg and then sharply increase at higher angles. Note that  $H_{on}$  has large errors for  $\theta$  above 70 deg due to broadening in field of the peak as the  $ab$  plane is approached.

The inset to Fig. 4 shows the same data as the main figure, but at 25 K and with more data points for  $H_{c2}(\theta)$ . Previously,<sup>9</sup>  $H_{c2}(\theta)$  in  $MgB_2$  was shown to deviate slightly from the anisotropic Ginzburg-Landau theory (AGLT).<sup>21</sup> This was explained within a dirty two-band superconducting model.<sup>22</sup> Differentiating between the AGLT and the two band model is beyond the scope of our experimental technique. Therefore, we cannot add a further contribution to this particular observation. Within the resolution of our experiment, AGLT provides a sufficient guide to the evolution of  $H_{max}(\theta)$  and  $H_{c2}(\theta)$  as shown by the full lines in the main figure and inset. Using this extrapolation, we estimate  $H_{c2\parallel ab}$  and calculate the anisotropy parameter for the upper critical field as  $\gamma \approx 2 \pm 0.5$  at both 20 and 25 K. The most significant observation is the completely different behavior of  $H_{on}(\theta)$  and  $H_{infl}(\theta)$  in comparison with the angular dependence of  $H_{c2}(\theta)$  and  $H_{max}(\theta)$ . This is in marked contrast to an earlier report on significantly less disordered crystals.<sup>8</sup>

A summary of  $H_{infl}(\theta)$  at 7, 10, 15, 20, and 25 K is shown in Fig. 5. As the temperature is decreased, two changes in  $H_{infl}(\theta)$  can be seen; the flat curve profile below 60 deg approaches the low temperature constant value of  $\sim 1.3$  T and the curve slope change above 60 deg becomes more sharply defined. The close lying curves reflect the very weak temperature dependence of the transition.

#### IV. DISCUSSION

The upper critical fields shown in Figs. 3 and 4 are approximately double the values measured immediately after irradiation,<sup>14</sup> and  $T_c$  has decreased from 38 to 36 K over the same period. The change in  $H_{c2}$  is a consequence of the

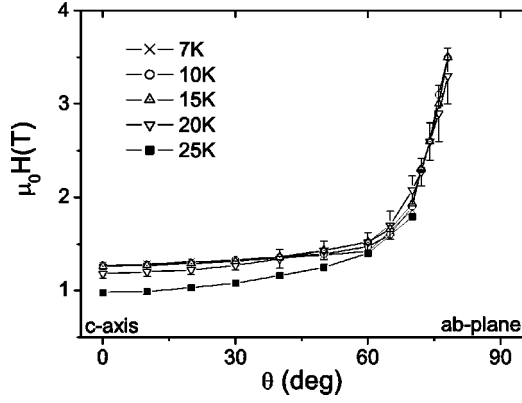


FIG. 5. The inflection point of the peak  $H_{\text{infl}}$  is shown as a function of the field angle  $\theta$  at several temperatures marked by the symbols in the legend

introduced disorder that resulted from the irradiation and subsequent aging. However, the anisotropy of the upper critical field in the virgin crystal<sup>12</sup> was  $\gamma=2.1\pm 0.1$ , which is similar to that measured for the 6 month aged sample of  $\gamma=2\pm 0.5$ . This suggests that the disorder responsible for the enhancement of  $H_{c2}$  is isotropic and has remained so as the sample has aged. Therefore, we are confident that the observed angular dependence of the order-disorder transition reflects intrinsic properties of the vortex lattice and does not reflect anisotropic disorder.

We interpret the presence of overshoot (undershoot) in the field decreasing (increasing) minor hysteresis loops  $\text{MHL}_{\downarrow}$  ( $\text{MHL}_{\uparrow}$ ) and the increased magnetic hysteresis in field-cooled MHLs when all compared to the zero-field cooled full  $M$ - $H$  loop (see Fig. 2) as demonstration of a first order order-disorder transition from a Bragg glass to a vortex glass.<sup>2-6</sup>

For such a disorder driven transition, Giller *et al.*<sup>5</sup> showed

$$H_{\text{on}}(T) \propto \xi^{-3} = H_{\text{on}}(0)[1 - (T/T_c)^4]^{3/2}, \quad (1)$$

where  $H_{\text{on}}(0)$  is the zero temperature value of the onset field to the peak and  $\xi$  is the coherence length. It relates the competition between the elastic energy of the vortex lattice and the pinning energy of the disorder and assumes the thermal energy is small in comparison, which is the case in  $\text{MgB}_2$ . Equation (1) is fitted to  $H_{\text{on}}(T)$  and  $H_{\text{infl}}(T)$  shown by the dotted lines in Fig. 3. The fit shows similar temperature independence to both data sets below 15 K, but underestimates the data at higher temperatures with the fit curve lying below the error bars for 25 K and above. The application of Eq. (1) to  $H_{\text{infl}}$  is justified by the similar temperature and angular dependence between  $H_{\text{on}}$  and  $H_{\text{infl}}$  seen in Figs. 3 and 4, respectively, and because they both occur within the field range of the magnetic history effects as illustrated in Fig. 2(c).

Scaling argument taken from AGLT<sup>21</sup> suggest that within the resolution of our experiment  $H_{c2}(\theta)$  follows the dependence

$$H_{c2}(\theta) = H_{c2\parallel c}/(\cos^2 \theta + \gamma_{hc2}^{-2} \sin^2 \theta)^{1/2}, \quad (2)$$

where  $\gamma_{hc2}$  is the upper critical field anisotropy parameter. On the other hand Eq. (1) shows that  $H_{\text{on}}(T)/H_{\text{infl}}(T)$  follow a  $\xi^{-3}$  dependence. There is no *a priori* reason that these two very different types of phase transition should have the same angular dependence on field and indeed in this highly disordered crystal we find that angular behavior is not the same. Other factors that could also affect the form of  $H_{\text{on}}(\theta)$  and  $H_{\text{infl}}(\theta)$  include any anisotropy in the elastic constants of the vortex lattice and the role of the two superconducting gaps on the structure of the vortex core.<sup>11</sup>

Angst *et al.*<sup>8</sup> observed the PE in native single crystal  $\text{MgB}_2$  and showed that  $H_{\text{on}}(T, \theta)$ ,  $H_{\text{max}}(T, \theta)$ , and  $H_{c2}(T, \theta)$  all fit similarly to AGLT, but  $H_{\text{on}}(T, \theta)$  was much closer to  $H_{c2}(T, \theta)$  than in our crystal. It should be noted that in the Angst *et al.* crystal the peak effect was present at all applied field angles. Our crystal is more heavily disordered and has an order-disorder transition at much lower fields and displays notably different temperature and field orientation dependence to the upper critical field.

## V. CONCLUSIONS

We have studied a heavily disordered  $\text{MgB}_2$  single crystal that shows a peak effect in the  $M$ - $H$  loop with a peak onset field that is significantly less than the value of  $H_{c2}$ . We have demonstrated that the vortex transition we have observed is likely to be that from a low field quasiordered state to a high field highly disordered phase. The transition displays significantly different temperature and field orientation dependence from both the upper and lower critical fields

We find that the inflection field  $H_{\text{infl}}$  near the onset of the peak is a suitable identifying point for the phase transition, and it is accompanied by magnetic history effects in the  $M$ - $H$  loops suggestive of a first order transition. The temperature dependence of  $H_{\text{infl}}$  fits Eq. (1) from Giller *et al.*<sup>5</sup> with a  $T$ -independent profile at low temperatures, but differs somewhat from that model at high temperatures where thermal effects might play a role. The most striking result is that the angular dependence  $H_{\text{infl}}(\theta)$  deviates strongly from the behavior of the upper and lower critical fields. It is also in marked contrast to that found in lightly disordered  $\text{MgB}_2$ .<sup>8</sup> This suggests that our heavily disordered crystal may represent a different pinning regime than has been previously observed with regard to the pinning-nucleated order-disorder transition.

## ACKNOWLEDGMENTS

The authors would like to thank Dr. S. B. Roy for useful discussions, and acknowledge financial support by the UK Engineering & Physical Sciences Research Council.

- <sup>1</sup>A. Schilling, R. A. Fisher, N. E. Phillips, U. Welp, D. Dasgupta, W. K. Kwok, and G. W. Crabtree, *Nature (London)* **382**, 791 (1996).
- <sup>2</sup>G. Ravikumar, V. C. Sahni, A. K. Grover, S. Ramakrishnan, P. L. Gammel, D. J. Bishop, E. Bucher, M. J. Higgins, and S. Bhattacharya, *Phys. Rev. B* **63**, 024505 (2001).
- <sup>3</sup>M. Marchevsky, M. J. Higgins, and S. Bhattacharya, *Nature (London)* **409**, 591 (2001).
- <sup>4</sup>S. B. Roy, P. Chaddah, and S. Chaudhary, *Phys. Rev. B* **62**, 9191 (2000).
- <sup>5</sup>D. Giller, A. Shaulov, R. Prozorov, Y. Abulafia, Y. Wolfus, L. Burlachkov, Y. Yeshurun, E. Zeldov, V. M. Vinokur, J. L. Peng, and R. L. Greene, *Phys. Rev. Lett.* **79**, 2542 (1997).
- <sup>6</sup>B. Khaykovich, E. Zeldov, D. Majer, T. W. Li, P. H. Kes, and M. Konczykowski, *Phys. Rev. Lett.* **76**, 2555 (1996).
- <sup>7</sup>H. Kupfer, G. Linker, G. Ravikumar, T. Wolf, A. Will, A. A. Zhukov, R. Meier-Hirmer, B. Obst, and H. Wuhl, *Phys. Rev. B* **67**, 064507 (2003).
- <sup>8</sup>M. Angst, R. Puzniak, A. Wisniewski, J. Jun, S. M. Kazakov, and J. Karpinski, *Phys. Rev. B* **67**, 012502 (2003).
- <sup>9</sup>A. Rydh, U. Welp, A. E. Koshelev, W. K. Kwok, G. W. Crabtree, R. Brusetti, L. Lyard, T. Klein, C. Marcenat, B. Kang, K. H. Kim, K. H. P. Kim, H.-S. Lee, and S.-I. Lee, *Phys. Rev. B* **70**, 132503 (2004).
- <sup>10</sup>M. Zehetmayer, M. Eisterer, J. Jun, S. M. Kazakov, J. Karpinski, B. Birajdar, O. Eibl, and H. W. Weber, *Phys. Rev. B* **69**, 054510 (2004).
- <sup>11</sup>H. J. Choi, D. Roundy, H. Sun, M. L. Cohen, and S. G. Louie, *Phys. Rev. B* **66**, 020513(R) (2002).
- <sup>12</sup>G. K. Perkins, J. Moore, Y. Bugoslavsky, L. F. Cohen, J. Jun, S. M. Kazakov, J. Karpinski, and A. D. Caplin, *Supercond. Sci. Technol.* **15**, 1156 (2002).
- <sup>13</sup>Y. Bugoslavsky, L. F. Cohen, G. K. Perkins, M. Polichetti, T. J. Tate, R. Gwilliam, and A. D. Caplin, *Nature (London)* **411**, 561 (2001).
- <sup>14</sup>G. K. Perkins, Y. Bugoslavsky, A. D. Caplin, J. Moore, T. J. Tate, R. Gwilliam, J. Jun, S. M. Kazakov, J. Karpinski, and L. F. Cohen, *Supercond. Sci. Technol.* **17**, 232 (2004).
- <sup>15</sup>D. Lacey, R. Gebauer, and A. D. Caplin, *Supercond. Sci. Technol.* **8**, 568 (1995).
- <sup>16</sup>D. Ertas and D. Nelson, *Physica C* **272**, 79 (1996).
- <sup>17</sup>V. Vinokur, B. Khaykovich, E. Zeldov, M. Konczykowski, R. A. Doyle, and P. H. Kes, *Physica C* **295**, 209 (1998).
- <sup>18</sup>T. Giamarchi and P. Le Doussal, *Phys. Rev. B* **55**, 6577 (1997).
- <sup>19</sup>S. Ooi, T. Tamegai, and T. Shibauchi, *Physica C* **259**, 280 (1996).
- <sup>20</sup>R. Yoshizaki, H. Ikeda, and D. S. Jeon, *Physica C* **225**, 299 (1994).
- <sup>21</sup>G. Blatter, V. B. Geshkenbein, and A. I. Larkin, *Phys. Rev. Lett.* **68**, 875 (1992).
- <sup>22</sup>A. A. Golubov and A. E. Koshelev, *Phys. Rev. B* **68**, 104503 (2003).